ACS Sustainable Chemistry & Engineering

pubs.acs.org/journal/ascecg

Research Article

Quasiliving Cationic Polymerization of Anethole: Accessing High-Performance Plastic from the Biomass-Derived Monomer

Maksim I. Hulnik, Olga V. Kuharenko, Irina V. Vasilenko, Peter Timashev, and Sergei V. Kostjuk*

Cite This: *ACS Sustainable Chem. Eng.* 2021, 9, 6841−6854

Read Online

ACCESS | Metrics & More | Article Recommendations | Supporting Information

ABSTRACT: Quasiliving cationic polymerization of the naturally occurring β-methylstyrene derivative, anethole, is reported for the first time. The effect of solvent polarity, initiator nature as well as Lewis acid, proton trap, and initiator concentrations on the cationic polymerization of anethole in the presence of $SnCl_4$ as a coinitiator was studied in detail. It was shown that $SnCl_4$-coinitiated cationic polymerization of anethole proceeds in a quasiliving fashion in the presence of different initiators (cumyl chloride, p-methoxystyrene−HCl, and dicumyl chloride) using 2,6-lutidine as a proton trap and toluene as a solvent at −50 and −60 °C affording poly(anethole)s with the number-average molecular weight up to 24,000 g mol^{-1} and relatively low polydispersity ($Đ$ = 1.25−1.51). The quasiliving nature of polymerization was confirmed by the linearity of first-order kinetic plot, linear increase of M_n with increasing conversion, as well as by monomer addition experiment. The analysis of size exclusion chromatography traces of the synthesized polymers revealed the presence of a high-molecular-weight fraction (from 9 to 20% depending on solvent polarity and temperature), which is generated due to competitive chain transfer to the monomer *via* its alkylation by growing macrocations and occurring simultaneously with propagation. The synthesized poly(anethole)s are characterized by a high value of glass transition temperature (T_g up to 255 °C), high thermal stability (T_{d5} = 386 °C), and high Young's modulus (3.1 ± 0.5 GPa) comparable with values for such commercially available plastics as polystyrene and poly(methyl methacrylate). In addition, the obtained polymer shows increased resistance to bacterial (*Escherichia coli*) growth on the polymer surface in comparison with polystyrene.

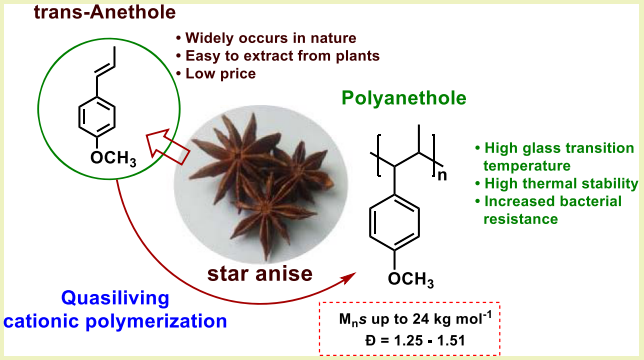

KEYWORDS: *naturally occurring monomer, anethole, quasiliving cationic polymerization, high-performance plastic*

INTRODUCTION

The depletion of fossil fuels and environmental concerns has been the main cause of rapidly growing interest in renewable resources for the last few decades. In particular, much attention in polymer chemistry has been devoted to the development of novel biobased polymers to replace petroleum-derived polymer materials.[1−10] A wide structural biodiversity of natural compounds endow specific properties and functions to polymers derived from such compounds that are not present in conventional synthetic polymers. Combined with the possibilities of quasiliving polymerization and/or post-polymerization modification, polymers from biobased raw materials have a high potential to be applied not only like common elastomers[11,12] or plastics[13,14] but also for specialized purposes, for instance, as absorbents,[15] self-healing materials,[16] scaffolds for tissue regeneration,[17,18] and so forth.

Anethole (An) is a naturally occurring vinyl compound that is abundantly contained in essential oils of various plants, such as fennel and star anise, and is annually extracted from them on a large scale for application in the flavor and fragrance industries.[19] Since anethole could be regarded as a β-methylstyrene bearing a methoxy group at para-position of an aromatic ring, the presence of an electron-donating substituent makes it possible to expect the reactivity of such compound in polymerization processes proceeding *via* cationic and radical mechanisms.[20] However, it is known that 1,2-disubstituted olefins exhibit little or no tendency to undergo homopolymerization due to a steric hindrance.[21,22]

In spite of low reactivity in polymerization processes, anethole, due to the presence of two reactive groups, is widely used to design new monomers and polymers.[23] Indeed, many anethole-based polymeric materials, such as heat-resistance materials,[24,25] dielectric materials,[26] and high-performance materials,[27,28] have been developed for the past 2 decades. However, the preparation of anethole-based monomers

Received: March 4, 2021
Revised: April 12, 2021
Published: May 3, 2021

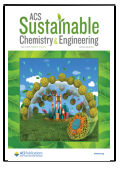

https://doi.org/10.1021/acssuschemeng.1c01504
ACS Sustainable Chem. Eng. 2021, 9, 6841−6854

typically require multistep synthetic procedures that increase significantly the price of the resulting polymers. Therefore, the design of new catalytic systems suitable for direct polymerization of anethole to construct diverse well-defined biobased polymers and block copolymers remains a challenging issue.

To the best of our knowledge, there are no publications on successful radical homopolymerization of anethole up to date. However, anethole can be radically copolymerized with vinyl monomers possessing electron-withdrawing substituents.[29−32] For example, free-radical copolymerization of anethole with maleic anhydride or terpolymerization of maleic anhydride, anethole, and isobutyl vinyl ether afforded copolymers with M_ns ≤ 10,000 g mol^{-1} and polydispersity in the range of 1.4−2.8.[30] High-molecular-weight copolymers (M_n up to 68,000 g mol^{-1}) with high T_gs (>100 °C) were synthesized *via* free-radical copolymerization of anethole with acrylic monomers (methyl-, *n*-butyl-, and *tert*-butylacrylates) in fluoroalcohols using α,α′-azoisobutyronitrile as a radical initiator.[32] Trithiocarbonate- and dithiobenzoate-mediated reversible addition−fragmentation transfer (RAFT) copolymerization of anethole and methyl acrylate performed in toluene and *m*-$C_6H_4[C(CF_3)_2OH]_2$ as solvents results in well-defined copolymers with the controlled molecular weight (M_n up to 10,000 g mol^{-1}) and low polydispersity ($Đ$ ≤ 1.2).[32] Cross-linked poly(anethole-*co*-maleic anhydride)s in the form of microspheres (about 1 μm in size) with high absorption ability can be obtained *via* the so-called "free-radical precipitate" polymerization.[33] Such biobased microspheres can be further modified to construct more complex macromolecular architectures with improved surface performance[15] and/or new functions.[34−36]

In view of the non-homopolymerizability of anethole *via* radical mechanism, cationic polymerization seems to be a single polymerization technique obviously suitable for preparing homopolymers from this naturally occurring vinyl monomer. Indeed, there are few reports on conventional cationic homopolymerization of anethole.[37−39] However, they described the preparation of ill-defined, mainly low-molecular-weight polymers[37,38] or even dimers or trimers.[39] Conventional cationic copolymerization of anethole with styrene and *p*-methoxystyrene (pMOSt) was also reported,[40,41] but the authors did not provide any data about molecular weight and polydispersity of the obtained copolymers. In 2007, Kamigaito *et al.* performed successful cationic alternating copolymerization of anethole and pMOSt with a pMOSt−OH/BF_3OEt_2 initiating system in the presence of water, affording well-defined copolymers with controlled molecular weight (M_n up to 12,000 g mol^{-1}) and relatively low polydispersity ($Đ$ = 1.2−1.4), whereas no homopolymerization of An occurred under the same conditions.[42] The copolymerization did not proceed in the absence of non-sterically hindered pMOSt, but the consumption of An resumed with a new batch of pMOSt feed.[42] Despite involving neat An into the copolymerization process, this approach suffers from the necessity of using expensive pMOSt as a comonomer.

In line with our interest in the synthesis of (co)polymers from renewable biomass resources, we have reported the cationic (co)polymerization of two representatives of terpenes, that is, β-myrcene[43] and β-pinene[44] under eco-friendly conditions. Thus, high-molecular-weight poly(β-myrcene)s (up to 150 kg mol^{-1}) and a series of random poly(β-myrcene-*co*-styrene)s (M_n from 60 to 120 kg mol^{-1}) were synthesized *via* aqueous cationic polymerization initiated by a water-dispersible Lewis acid−surfactant-combined (LASC) catalyst.[43] The cationic polymerization of β-pinene affording relatively high-molecular-weight polymers (M_n = 9000−14,000 g mol^{-1}) with good thermal properties (T_g = 82−87 °C) was performed at room temperature using complexes of $AlCl_3$ with ethers in toluene as a solvent.[44]

In the present work, we report for the first time the quasiliving cationic polymerization of anethole, a biomass-derived monomer, using different initiators [cumyl chloride (CumCl), pMOSt−HCl, or dicumyl chloride (DiCumCl)] in conjunction with $SnCl_4$ as a coinitiator and 2,6-lutidine as a proton trap in toluene as a solvent at −50 or −60 °C (Scheme 1). Poly(anethole)s (PAns) with controlled molecular weight

Scheme 1. Quasiliving Cationic Polymerization of Anethole

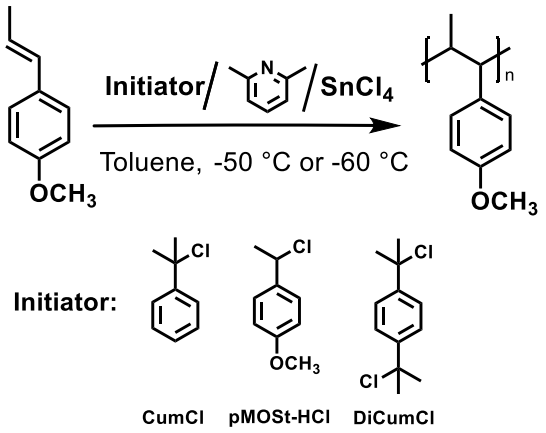

up to 24,000 g mol^{-1} and relatively low polydispersity ($Đ$ = 1.25−1.51) were synthesized, although the polymerization was accompanied by the side reaction of monomer alkylation by macrocations resulting in the generation of some amount of high-molecular-weight fraction (ω = 9−20%). The synthesized PAs displayed high glass transition temperature values (T_g > 210 °C), excellent thermal stability (T_{d5} = 386 °C), and high Young's modulus 3.1 ± 0.5 GPa. A brief microbiological test was also performed in the study, revealing the reduced adhesion of *Escherichia coli* cells on PAn surface as compared to that of polystyrene (PSt).

EXPERIMENTAL SECTION

Materials. *trans*-Anethole (Sigma-Aldrich, 99%), pMOSt (Sigma-Aldrich, 97%), and 2,6-lutidine (Merck, 98%) were distilled before using over calcium hydride (CaH_2) under reduced pressure and stored in a dry argon atmosphere. 2,6-Di-*tert*-butylpyridine (DTBP, Sigma-Aldrich, 97%), $SnCl_4$ (Aldrich, 99.999%), methanesulfonic acid (MSA, Sigma-Aldrich, 99%), tetrabutylammonium bromide (Sigma-Aldrich, 98%), tetrahydrofuran (THF) (for liquid chromatography, Sigma-Aldrich), ethanol (Sigma-Aldrich, 96%), and $CDCl_3$ (Eurisotop) were used as received. Toluene (Tol, Sigma-Aldrich, 99.8%) was dried by refluxing with Na followed by distilling under an argon atmosphere. Dichloromethane (Sigma-Aldrich, 99.8%) was refluxed and distilled over CaH_2 under an argon atmosphere. 2-Chloro-2-phenylpropane (CumCl) was prepared by passing dry HCl gas through α-methylstyrene solution in solvent mixture Hex/CH_2Cl_2 [1:2:1 α-methylstyrene/Hex/CH_2Cl_2 (v/v/v)] at 0 °C for 2 h. Then, dry argon was bubbled to remove excess of unreacted HCl for 5 h. Finally, after removing the solvent by evaporation, the product was purified by distillation with CaH_2 under reduced pressure. 1-Chloro-1-(*p*-methoxyphenyl)ethane (pMOSt−HCl) was synthesized by a similar method: dry hydrogen chloride was bubbled into pMOSt in CH_2Cl_2 [1:10 pMOSt/CH_2Cl_2 (v/v)] at −78 °C, and then dry argon was bubbled to remove unreacted HCl. CH_2Cl_2 was removed using a

https://doi.org/10.1021/acssuschemeng.1c01504
ACS Sustainable Chem. Eng. 2021, 9, 6841−6854

Table 1. Cationic Polymerization of Anethole with the CumCl/$SnCl_4$ Initiating System at −30 °C in Different Solvents[a]

entry	solvent	$SnCl_4$ (mM)	time (min)	conv. (%)	$M_{n,theor}$[b] (g mol^{-1})	M_n[c] (g mol^{-1})	$Đ$[c]	M_n[d] (kg mol^{-1})	$Đ$[d]	ω[e](%)
1	CH_2Cl_2	8	5	100	11,300	[f]	[f]	[f]	[f]	[f]
2[g]	CH_2Cl_2	4	2	76	8,600	4,800	1.53	173	1.90	30
3	CH_2Cl_2/toluene[j]	8	30	81	9,130	8,700	1.66	131	1.38	26
4	toluene	10	120	58	6,540	8,240	1.56	91	1.12	4
5[h]	toluene	10	120	74	8,400	9,000	1.70	105	1.17	8
6[h,i]	toluene	10	50	98	11,050	11,500	1.31	129	1.40	20

[a]Polymerization conditions: [An] = 0.15 M; [CumCl] = 2 mM; [DTBP] = [2,4-lutidine] = 4 mM. [b]$M_{n,theor}$ = ([An]/[CumCl] × 148.2 × conv. + M_r(CumCl)). [c]For low-molecular-weight fraction. [d]For high-molecular-weight fraction. [e]ω represents the content of the high-molecular-weight fraction calculated from SEC curves. [f]Polymer is insoluble in common organic solvents. [g][DTBP] = 2 mM. [h]2,6-Lutidine was used as a proton trap instead of DTBP. [i]T = −60 °C. [j]CH_2Cl_2/toluene 50:50 v/v.

vacuum pump. 1,4-Bis(2-chloro-2-propyl)benzene (DiCumCl) was synthesized according to the described method[45] *via* passing gaseous HCl through a solution of 1,4-bis(2-hydroxyisopropyl)benzene in methylene chloride at 0 °C. Then, the product of the synthesis was twice recrystallized from *n*-hexane and dried in vacuum. The purity of the synthesized initiators (>98%) was confirmed by ^{1}H NMR spectroscopy.

Polymerization Procedure. All operations were performed in a dry argon atmosphere. In a typical experiment, toluene (14.2 mL), anethole (0.34 mL), and 2,6-lutidine (7 μL) were sequentially charged into a Schlenk tube at room temperature. After the reactor was cooled to a necessary temperature (from −30 to −70 °C), an initiator (0.3 mL of 0.1 M solution of CumCl in toluene) was added to the reaction mixture. In experiments with DiCumCl, the calculated amount of the initiator was initially charged as a solid to the reactor. The polymerization was initiated by adding 1 M solution of $SnCl_4$ in toluene (0.15 mL). After a predetermined time, 1.5−2 mL aliquots were withdrawn and poured into an excess of ethanol. The precipitated polymer was further separated from the solution by centrifugation and dried in vacuum. Monomer conversions were determined gravimetrically. For the analyses, polymers were preliminarily dissolved in $CHCl_3$, precipitated in an excess of ethanol, and then dried in vacuum.

Instrumental Methods. Size exclusion chromatography (SEC) was performed on an UltiMate 3000 Thermo Scientific apparatus with Agilent PLgel 5 μm MIXED-C (300 × 7.5 mm) column and one precolumn (PLgel 5 μm guard 50 × 7.5 mm) thermostated at 30 °C. The detection was achieved by a differential refractometer (RI) as well as a diode array detector (UV). THF was eluted at a flow rate of 1.0 mL/min. The calculation of molar mass and polydispersity was carried out using PSt standards (Polymer Labs, Germany).

^{1}H spectra were recorded in $CDCl_3$ at 25 °C on a Bruker AC-500 spectrometer calibrated relative to the residual solvent resonance.

Matrix-assisted laser desorption−ionization time-of-flight mass spectrometry (MALDI-TOF MS) was performed on a Voyager mass spectrometer (AB Sciex). The instrument is equipped with a pulsed N_2 laser (337 nm) and a time-delayed extracted ion source. The spectra were recorded in the positive-ion mode using the reflectron and with an accelerating voltage of 20 kV. Solutions of dithranol (20 mg/mL) (Alfa Aesar, 1,8,9-anthracenetriol 97+%), the polymer sample (10 mg/mL), and sodium iodide (Aldrich, 99.9%) (10 mg/mL) were prepared in THF (Aldrich, 99.9%). These solutions were then mixed in the ratio of matrix/sample/cationizing salt = 10:2:1, and 0.5 μL aliquots were applied to a MALDI sample target for analysis. The instrument was calibrated externally using poly(ethylene glycol) standards at the appropriate molar mass. All mass-to-charge ratios (m/z) quoted are monoisotopic, that is, they include the most abundant isotopes of the elements present in the corresponding ion.

Density functional theory (DFT) calculations have been carried out using the DFT B3LYP method.[46] The geometries of the investigated molecules were fully optimized with the 6-31G(d) basis set. In order to perform stationary point characterization, vibrational frequencies were calculated for the structures obtained at the B3LYP/6-31G(d) level. The solvent effects were evaluated using the polarized continuum model[47] with the default parameters for toluene. The cavity was built up using a united atom model. Further single-point calculations including natural bond orbital (NBO) analysis were performed at the B3LYP/6-311+G(d,p) level of theory.

Differential scanning calorimetry (DSC) and thermogravimetric analysis (TGA) measurements were carried out using a Netzsch STA (simultaneous thermal analysis) 449 F3 device. The phase and relaxation transitions of the polymer were studied in the range of 30−300 °C with a heating/cooling rate of 10 °C min^{-1} in helium gas flow. The first and second heating cycles were examined in thermograms. The glass transition temperature (T_g) was evaluated by analyzing the inflection point from the second cycle. TGA was performed by heating polymer samples from 30 to 600 °C at the rate of 10 °C min^{-1} in nitrogen flow.

Nanomechanical measurements were performed on a BioScope Resolve atomic force microscopy (AFM) (Bruker, Santa Barbara, CA) system mounted on an Axio Observer inverted optical microscope (Carl Zeiss, Germany). The polymer films were prepared from a 2% solution of poly(anethole) in $CHCl_3$. The TAP525 silicon cantilevers (Bruker, Santa Barbara, CA) were used with the nominal spring constant of 200 N/m and the nominal tip radius of 8 nm. The exact value of the spring constant was determined by the thermal tune method, and the tip radius was measured after scanning the titanium roughness sample using NanoScope Analysis software (Bruker, Santa Barbara, CA). All AFM measurements were performed in air at room temperature. Force volume mapping was performed over 10 × 10 μm^2 areas with 16 × 16 force curve arrays. Three samples of each film and at least five areas per sample were analyzed. The vertical piezo movement speed was 12 μm/s, and the trigger force was ≈3 μN providing an indentation depth of 5−10 nm. The force volume maps were analyzed in NanoScope Analysis software to extract the indentation (Young's) modulus values using the Hertz model (paraboloid indenter)

$$F = \frac{4}{3}\frac{E}{1-\nu^2}\sqrt{R}\delta^{3/2} \quad (1)$$

where F is the measured force, E is the Young's (indentation) modulus, ν is the Poisson ratio (assumed to be 0.3), R is the tip radius, and δ is the indentation depth. The E values were averaged over each map and then over all maps of each sample; the values are presented as the mean ± standard deviation.

For microbiological tests, Gram-negative bacteria *E. coli* (strain M17) were cultivated in lysogeny broth (LB) medium. After cultivation for 24 h, bacteria were suspended in fresh LB medium (initial A600 was 0.1). Then, 1.0 mL aliquots of the suspension were charged over experimental polymer films placed into 24-well plate wells and cultivated for 24 h at 37 °C with a mixing rate of 200 rpm (ES20, Biosan, Latvia). Then, the polymer film surfaces were investigated using optical microscopy (Levenhuk 740T, Levenhuk, Russia).

RESULTS AND DISCUSSION

Cationic polymerization of An was initially investigated using CumCl/$SnCl_4$/DTBP initiating system due to the high

https://doi.org/10.1021/acssuschemeng.1c01504
ACS Sustainable Chem. Eng. 2021, 9, 6841−6854

efficiency of this initiating system in quasiliving cationic polymerization of pMOSt,[48] a structurally similar monomer to An (Table 1).

In conditions similar to the ones used for the pMOSt polymerization ([M] = 0.15 M; [$SnCl_4$] = 8 mM; [DTBP] = 4 mM; CH_2Cl_2; −30 °C),[48] the polymerization of An was completed in 5 min, affording PAn in a quantitative yield but totally insoluble in common organic solvents such as methylene chloride and THF (Table 1). The decrease in $SnCl_4$ concentration and reaction time allows obtaining polymers fully soluble in organic solvents, which are characterized by lower than theoretical molecular weight (entry 2, Table 1) as well as by the presence of a high molecular fraction of about 25−30% (Figure 1, Table 1). This

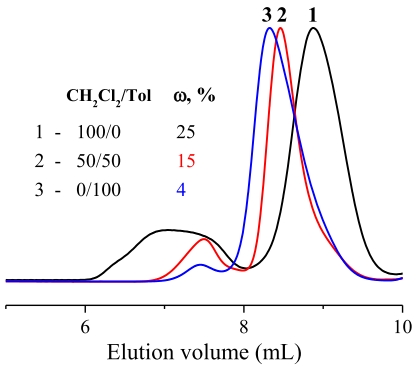

Figure 1. Gel permeation chromatography traces of PAns synthesized in the presence of a CumCl/$SnCl_4$/DTBP initiating system in different solvents at similar monomer conversions (~60%). Solvents: (1) CH_2Cl_2/Tol = 100/0 (entry 1, Table S1); (2) CH_2Cl_2/Tol = 50/50 (entry 2, Table S1), and (3) CH_2Cl_2/Tol = 0/100 (entry 3, Table S1). The content of the high-molecular-weight fraction calculated from SEC curves is represented by "*ω*".

result probably suggests that intermolecular alkylation proceeds during the cationic polymerization of anethole or under monomer-starved conditions. This side reaction did not occur in the case of pMOSt polymerization; however, the latter process was observed for the $TiCl_4$-coinitiated cationic polymerization of styrene.[49−51] Alternatively, the presence of two types of active species (ion pairs and free ions) could be responsible for the observed bimodal molecular weight distribution.[52−56]

In order to verify the last assumption, the effect of ammonium salt (Bu_4NBr) on the cationic polymerization of anethole was investigated. Indeed, this approach is widely used in cationic polymerization of styrene and its derivatives in polar solvent for suppressing propagation *via* free ions by shifting equilibrium between propagating (active) and non-propagating (dormant) species toward the latter.[52−56] This, in turn, allows converting the conventional cationic polymerization into a quasiliving one. However, the CumCl/$SnCl_4$/Bu_4NBr initiating system induced only slow polymerization of anethole, which was terminated at incomplete monomer conversion (conv. < 40%) (Table S2). The number-average molecular weight of synthesized polymers did not change with the monomer conversion, while polydispersity was relatively high (*Đ* = 1.4−1.7). Moreover, the high-molecular-weight fraction did not disappear upon Bu_4NBr addition, indicating that side reactions, not a presence of free ions, are most probably responsible for the generation of the high-molecular-weight fraction in An polymerization (Table S2).

In strong contrast to the addition of salt, the decrease of the solvent polarity *via* substitution of CH_2Cl_2 by toluene results in an anticipated decrease of the reaction rate, on the one hand. On the other hand, the experimental values of molecular weight become close to theoretical ones, while the content of the high-molecular-weight fraction decreases (down to 4%) with the increasing fraction of toluene in the solvent mixture (see entries 1−4 in Table 1). This positive effect of toluene on the control of cationic polymerization of anethole cannot be explained by a simple decrease of the solvent polarity in a view of inefficiency in controlling the polymerization by the addition of ammonium salt (*vide supra*). Indeed, the decrease of solvent polarity, similar to the addition of ammonium salt in a polar solvent, leads to a shift of equilibrium between active and dormant species toward the latter.[57] Therefore, the function of toluene consists of the formation of a complex with the Lewis acid and possible interaction with growing species as it was shown earlier for the cationic polymerization of isobutylene[58,59] and *β*-pinene.[60] This allows modifying the acidity of Lewis acid and stabilizing growing species that results in the suppression of the side reactions and, in turn, proceeding the polymerization in a quasiliving fashion.

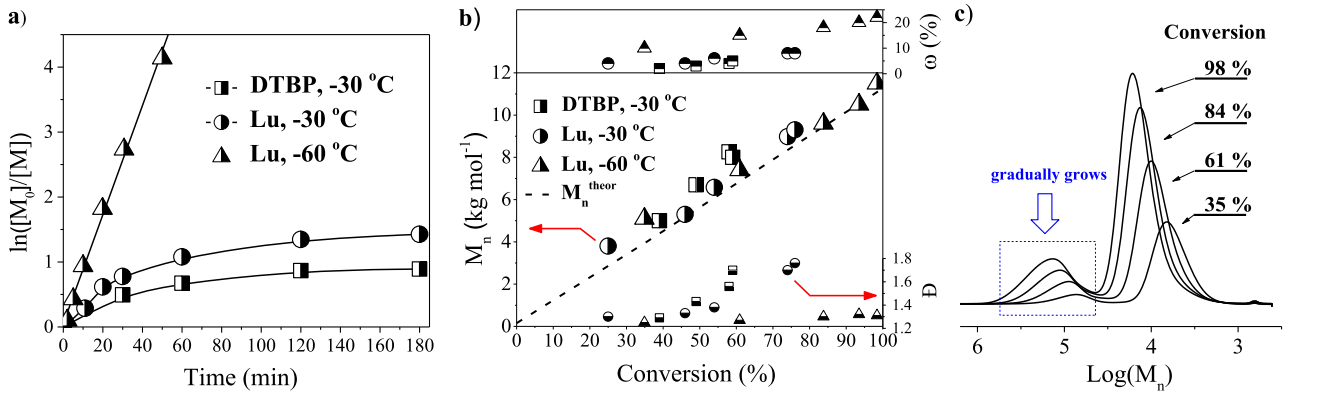

Figure 2. (a) First-order kinetic plots and (b) M_n, *Đ* (for low-molecular-weight fraction) and the content of high-molecular-weight fraction (*ω*) *vs* conversion dependences for the cationic polymerization of anethole with the CumCl/$SnCl_4$ initiating system in toluene in the presence of different proton traps (DTBP; 2,6-lutidine) at various temperatures (−30; −60 °C): [An] = 150 mM; [CumCl] = 2 mM; [$SnCl_4$] = 10 mM; [proton trap] = 4 mM. (c) SEC traces for the PAns synthesized using 2,6-lutidine as a proton trap at −60 °C at different conversions.

https://doi.org/10.1021/acssuschemeng.1c01504
ACS Sustainable Chem. Eng. 2021, 9, 6841−6854

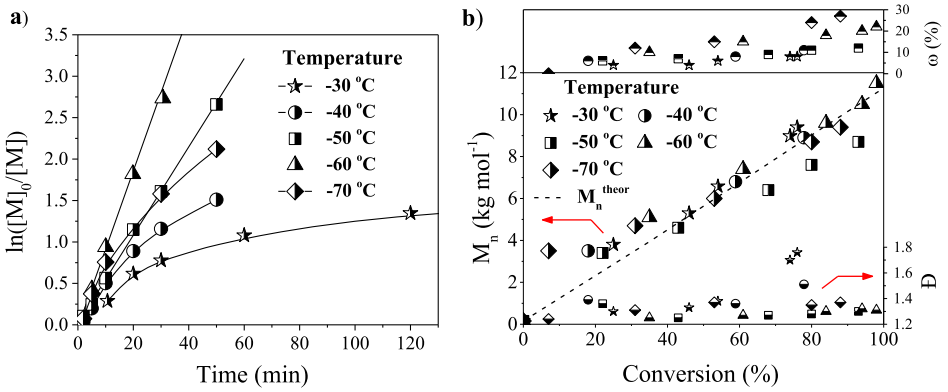

Figure 3. (a) First-order kinetic plots and (b) M_n, $Đ$ (for low-molecular-weight fraction) and the content of high-molecular-weight fraction (ω) *vs* conv. dependences for cationic polymerization of anethole using the CumCl/$SnCl_4$/2,6-lutidine initiating system in toluene at different temperatures: [An] = 150 mM; [CumCl] = 2 mM; [$SnCl_4$] = 10 mM; [2,6-lutidine] = 4 mM.

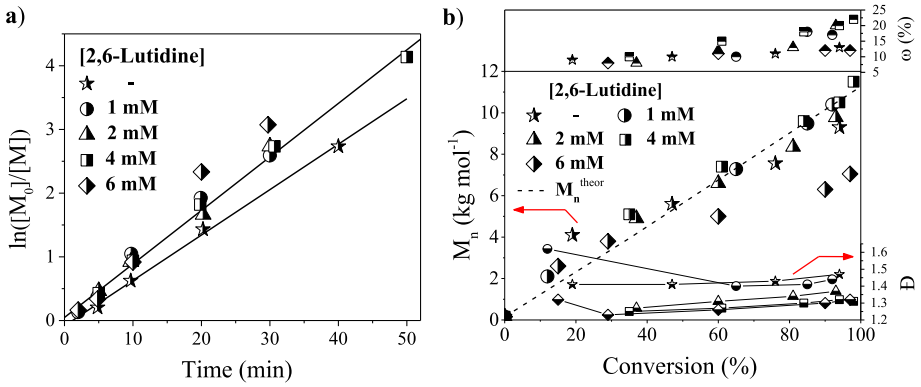

Figure 4. (a) First-order kinetic plots and (b) M_n, $Đ$ (for low-molecular-weight fraction) and the content of high-molecular-weight fraction (ω) *vs* conversion dependences for the cationic polymerization of anethole using the CumCl/$SnCl_4$/2,6-lutidine initiating system in toluene at different proton trap concentrations: [An] = 150 mM; [CumCl] = 2 mM; [$SnCl_4$] = 10 mM; and T = −60 °C.

However, despite significant enhancing of the controllability of An polymerization in toluene, the monomer conversion remained incomplete at −30 °C in the presence of the CumCl/$SnCl_4$/DTBP initiating system, even after 2 h (entry 4, Table 1). Taking into account that substitution of DTBP by much cheaper 2,6-lutidine (Lu) results in a somewhat higher polymerization rate in conjunction with the formation of a polymer with M_n closer to the theoretical one (entries 4 and 5, Table 1, Figure 2a), we used Lu in the further polymerization experiments. Importantly, the decrease of temperature from −30 to −60 °C resulted in complete monomer consumption and the synthesis of PAn with well-controlled M_n and relatively low polydispersity ($Đ \leq 1.30$) (Table 1).

In order to confirm the quasiliving nature of the cationic polymerization of anethole with the CumCl/$SnCl_4$/proton trap initiating system, kinetic investigations were then performed (Figure 2a). Indeed, the first-order plots are linear only for the polymerization performed at −60 °C, while significant deviation was observed for polymerization runs at higher temperatures, and the process was terminated at incomplete monomer conversion (Figure 2a). Although the experimental values of M_n were close to the theoretical line, the polydispersity remained relatively high and increased with increasing monomer conversion (Figure 2b), indicating that the polymerization is not quasiliving at −30 °C. This behavior is attributed to terminative chain transfer, when β-proton eliminated from growing macrocations is instantaneously and irreversibly entrapped by a proton trap.[61] In contrast, for polymerization of anethole performed at −60 °C along with the linearity of first-order plot, the linear increase of M_n with conversion and good correlation between experimental values of M_n and theoretical ones in conjunction with low polydispersity ($Đ \leq 1.3$) were observed (Figure 2b). In addition, SEC traces shifted to a high-molecular-weight region with the monomer conversion with no tailing in the low-molecular-weight region (Figure 2c). All these data confirm that polymerization of anethole with the CumCl/$SnCl_4$/2,6-lutidine initiating system proceeded in a quasiliving fashion at −60 °C. However, the high-molecular-weight fraction is still present in the polymer even at low monomer conversions, and its content increases gradually with increasing monomer conversion (Figure 2c). Therefore, the side reaction leading to the formation of the high-molecular-weight fraction proceeds not only under monomer-starved conditions but is also occurring in the course of polymerization, which is not consistent with features of intermolecular alkylation observed earlier in cationic polymerization of styrene.[62]

Aiming at defining the optimal reaction conditions for conducting the quasiliving cationic polymerization of anethole with the CumCl/$SnCl_4$ initiating system as well as elucidating the origin of the side reaction, the effects of temperature as well as Lewis acid, 2,6-lutidine, and initiator concentrations were further investigated.

Effect of Temperature. The detailed investigation of the influence of reaction temperature on the cationic polymerization of anethole using the CumCl/$SnCl_4$/2,6-lutidine

https://doi.org/10.1021/acssuschemeng.1c01504
ACS Sustainable Chem. Eng. 2021, 9, 6841−6854

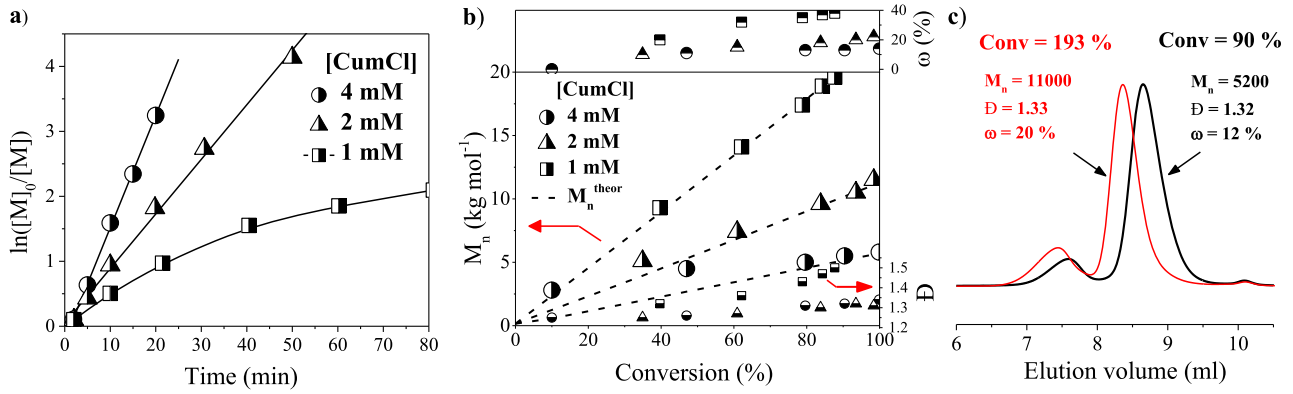

Figure 5. (a) First-order kinetic plots and (b) M_n, $Đ$ (for low molecular weight fraction) and the content of high-molecular-weight fraction (ω) *vs* conversion dependences for the cationic polymerization of anethole using the CumCl/$SnCl_4$/2,6-lutidine initiating system in toluene at different initiator concentrations: [An] = 150 mM; [$SnCl_4$] = 1 mM; [2,6-lutidine] = 4 mM; and T = −60 °C. (c) Additional monomer feed experiment for cationic polymerization of anethole at [CumCl] = 4 mM.

initiating system revealed nonlinearity of the first-order plots as well as increase of polydispersity with monomer conversion for polymerizations performed at temperatures higher than −40 °C (Figure 3), indicating that the process is not quasiliving under these conditions.

The quasiliving cationic polymerization of anethole proceeds at temperatures between −50 and −70 °C: the first-order plots are linear, M_n increases in direct proportion to monomer conversion, and polydispersity remains low through the polymerization (Figure 3). However, polymerization becomes slower at −70 °C, and the content of the high-molecular-weight fraction is strongly increased with decreasing temperature (Figure 3). Besides, the experimental values of M_n are located below the theoretical line when polymerization was performed at −50 °C (Figure 3b). Therefore, the optimal temperature for conducting the quasiliving cationic polymerization of anethole with the CumCl/$SnCl_4$/2,6-lutidine initiating system in toluene as a solvent is −60 °C.

Effect of Proton Trap Concentration. In order to find the optimal concentration of 2,6-lutidine (Lu), a series of polymerization experiments with varying concentrations of the proton trap (from 0 to 6 mM) were carried out in toluene at −60 °C. As depicted in Figure 4a, the reaction rate does not depend on the concentration of the proton trap and is slightly lower in the case of polymerization without addition of Lu [$k_{p,app}$ = 0.082 min^{-1} (with Lu) and $k_{p,app}$ = 0.071 min^{-1} (without Lu)]. Although the molecular weight increased with increasing monomer conversion for polymers synthesized without a proton trap, the experimental values of M_n are located below the theoretical line, while polydispersity is relatively high ($Đ \sim 1.5$) (Figure 4b). The addition of Lu results in a perfect correlation between experimental and theoretical values of molecular weight as well as in a significant decrease of polydispersity from $Đ \sim 1.50$ to $Đ \sim 1.25$ in the absence and presence of the proton trap, respectively (Figure 4b). However, at high Lu concentration (6 mM), a significant deviation of experimental values of M_n from the theoretical line is observed (Figure 4b), indicating that the proton trap at a relatively high concentration can act as a chain-transfer agent, abstracting protons from β-position toward growing macrocations.[63,64] Indeed, it was reported recently that the addition of a proton trap to $B(C_6F_5)_3$-coinitiated polymerization of pMOSt, a structurally similar monomer to anethole, results in the decrease of molecular weight of the synthesized polymers.[64] Therefore, based on the obtained results the optimal concentration of 2,6-lutidine as a proton trap was determined as 4 mM, which was used in further experiments. Interestingly, the addition of a proton trap along with improving control over polymerization also leads to some increase of the content of the high-molecular-weight fraction (Figure 4b).

Effect of Initiator Concentration. The study on the influence of initiator concentration on the kinetics as well as molecular weight and polydispersity evolution with monomer conversion was performed in order to estimate the scope and limitation of using the CumCl/$SnCl_4$/2,6-lutidine initiating system in the synthesis of well-defined PAns. As shown in Figure 5a, the reaction rate gradually decreased with the decrease in initiator concentration. The number-average molecular weight increased with increasing monomer conversion and experimental values of M_n correlated well with theoretical ones, while M_n was inversely proportional to the concentration of the initiator (Figure 5b). However, the first-order plot deviates from linearity for polymerization performed at the lowest concentration of the initiator studied ([CumCl] = 1 mM), whereas the polydispersity increases with the increase in monomer conversion and the content of the high-molecular-weight fraction is rather high (up to 40%) (Figure 5b). Therefore, well-defined PAns with controlled molecular weights ($M_n \leq$ 20,000 g mol^{-1}) could be prepared *via* cationic polymerization of anethole with the CumCl/$SnCl_4$/2,6-lutidine initiating system using an appropriate concentration of the initiator (2−4 mM).

In addition, the stability of growing macrocations and the possibility to synthesize the block copolymers were briefly estimated by the monomer addition experiment. In this experiment, the fresh batch of anethole was added to the reaction mixture when the initial charge had been almost completely consumed. The fresh batch of monomer was consumed somewhat slower in comparison to the initial one (Figure S1). This observation can be explained by the dilution of the reaction mixture since the second feed of monomer was charged into the reactor as a mixture with toluene [An/Tol = 1/3 (v/v)] due to the high melting point of anethole (T_m = 22.5 °C).[65] As it is shown in Figure 5c, the addition of the second feed of monomer leads to an increase in the molecular weight as well as shifting SEC traces into a high-molecular-weight region without detectable tailing, while the polydisper-

https://doi.org/10.1021/acssuschemeng.1c01504
ACS Sustainable Chem. Eng. 2021, 9, 6841−6854

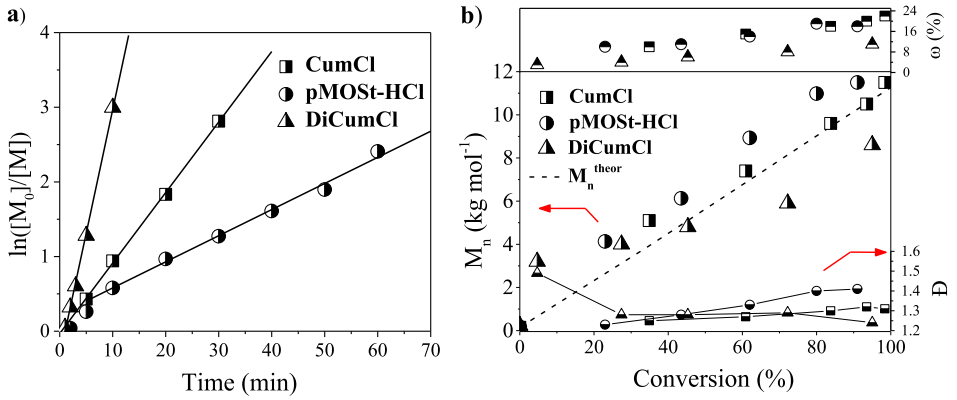

Figure 6. (a) First-order kinetic plots and (b) M_n, $Đ$ (for low-molecular-weight fraction) and the content of high-molecular-weight fraction (ω) *vs* conversion dependences for the $SnCl_4$-coinitiated cationic polymerization of anethole in toluene in the presence of different initiators: [An] = 150 mM; [initiator] = 2 mM; [$SnCl_4$] = 10 mM; [2,6-lutidine] = 4 mM; and T = −60 °C.

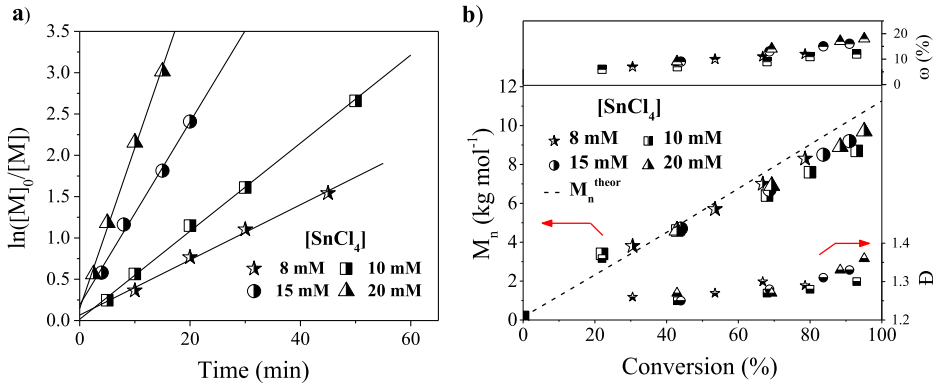

Figure 7. (a) First-order kinetic plots and (b) M_n, $Đ$ (for low-molecular-weight fraction) and the content of high-molecular-weight fraction (ω) *vs* conversion dependences for the $SnCl_4$-coinitiated cationic polymerization of anethole in toluene at different Lewis acid concentrations: [An] = 150 mM; [CumCl] = 2 mM; [2,6-lutidine] = 4 mM; and T = −50 °C.

sity does not change during the polymerization of the second portion of anethole (Figures 5c and S1). In turn, the content of the high-molecular-weight fraction increases almost twice (up to 20%) at the second stage (Figure S1) and takes the values close to the ones observed for PAn synthesized in a typical experiment (entry 6, Table 1). It should be noted that the high-molecular-weight fraction could be efficiently separated from the low-molecular-weight fraction by preparative chromatography, giving expected monomodal distribution for the last one (Figure S2).

Effect of Initiator Nature. With the aim of improving the controllability of the process as well as for better understanding of the polymerization mechanism through analysis of chain-end structure of the prepared polymers, the $SnCl_4$-coinitiated cationic polymerization of anethole was investigated in the presence of different initiators: MSA, an adduct of pMOSt with HCl (pMOSt−HCl), and DiCumCl (see Scheme 1). The MSA/$SnCl_4$ initiating system afforded conventional cationic polymerization of anethole with visible acceleration of monomer consumption during polymerization process, probably, due to slow ionization of initiator by Lewis acid (Figure S3). As a result, PAn with considerably higher than theoretical molecular weight (M_n = 19,000 g mol^{-1}, $M_{n,theor}$ = 5670 g mol^{-1}) and high polydispersity ($Đ$ = 1.96) containing a large fraction of insoluble polymer (up to 30%) was obtained (Table S3, Figure S4). These facts together with a much higher value of M_n for the high-molecular-weight fraction as compared to a polymer prepared with other initiators indicate the occurring of intensive side reactions in the case of using MSA as the initiator (Table S3). Surprisingly, the polymerization of anethole with pMOSt−HCl as the initiator proceeded almost 3 times slower than with CumCl ($k_{p,app}$ = 0.035 min^{-1} and $k_{p,app}$ = 0.094 min^{-1}, respectively) (Figure 6a) which is opposite to the activity of structurally similar alcohols in BF_3OEt_2-coinitiated cationic polymerization of styrene.[66] This observation could be tentatively attributed to partial initiator decomposition in the course of initiation/cationation. Such decomposition of CumCl was observed earlier for the isobutylene polymerization in the presence of acidic ionic liquids as co-initiator at relatively high reaction temperatures.[59] Indeed, although the first-order plots are linear for cationic polymerization of anethole with the pMOSt−HCl/$SnCl_4$ initiating system at different initiator concentrations (Figures 6a and S5), the experimental values of M_n are higher than theoretical ones, while polydispersity is relatively high (Figure 6b, Table S4). These data indicate that some decomposition of the initiator may indeed occur under investigated conditions.

Finally, DiCumCl in conjunction with $SnCl_4$ as the initiator and 2,6-lutidine as a proton trap was tested in cationic polymerization of anethole. As it could be expected, the difunctional initiator promoted significantly faster polymerization compared to CumCl and pMOSt−HCl ($k_{p,app}$ = 0.331 min^{-1} *vs* $k_{p,app}$ = 0.094 min^{-1} and $k_{p,app}$ = 0.035 min^{-1}, respectively). However, despite the linearity of the first-order

https://doi.org/10.1021/acssuschemeng.1c01504
ACS Sustainable Chem. Eng. 2021, 9, 6841−6854

kinetic plot, low polydispersity ($Đ$ = 1.24−1.28), and relatively low content of the high-molecular-weight fraction (ω < 12%), a poor control on molecular weight of the synthesized PAns was observed in the polymerization at −60 °C (Figure 6). Nevertheless, the quasiliving cationic polymerization of anethole with DiCumCl as the initiator was performed at −50 °C affording polymers with controlled M_n up 10,200 g mol^{-1}, the lowest polydispersity ($Đ \leq 1.25$) and the lowest content of the high-molecular-weight fraction ($\omega \leq 8\%$) among all initiators studied (Figure S6). The living nature of the DiCumCl-initiated cationic polymerization of anethole at −50 °C was also confirmed by monomer addition experiment (Figure S7). The experiments performed at different DiCumCl initiators showed that first-order plots remain linear up to [DiCumCl] = 1 mM, while some deviation from linearity was observed at lower initiator concentration (Figure S6a) as in the case of using CumCl as the initiator (Figure 5a). The number-average molecular weight increased with increasing monomer conversion, while M_n was inversely proportional to the concentration of the initiator (Figure S6b). However, the experimental values of M_n are located below the theoretical line for polymerizations performed at low initiator concentrations (Figure S6b), which may indicate the operating of side reactions.

Effect of $SnCl_4$ Concentration. To establish the nature of counterion/Lewis acid (monomeric or dimeric), which participates in initiating and propagating steps of $SnCl_4$-coinitiated cationic polymerization of anethole, the effect of the concentration of Lewis acid on the reaction rate and polymer properties was briefly investigated. As expected, the rate of polymerization increases with increasing concentration of $SnCl_4$ (Figure 7a). The first-order plots are linear at all $SnCl_4$ concentrations (Figure 7a). The M_n of the polymers increases in direct proportion to monomer conversion, while experimental values of molecular weight correlate well with a theoretical line at all $SnCl_4$ concentrations (Figure 7b).

The plot of $\ln(k_{p,app})$ versus $\ln[SnCl_4]$ gives a slope of nearly 2 (Figure 8), suggesting a second-order dependence on $SnCl_4$

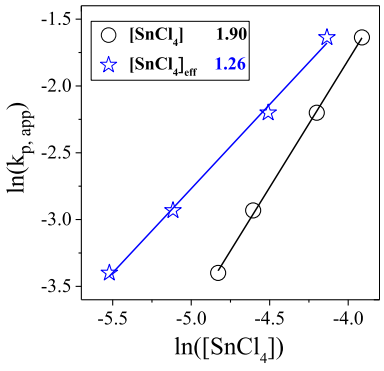

Figure 8. $\ln(k_{p,app})$ *vs* $\ln[SnCl_4]$ dependence for $SnCl_4$-coinitiated cationic polymerization of anethole in toluene: [An] = 150 mM; [CumCl] = 2 mM; [2,6-lutidine] = 4 mM; T = −50 °C. $[SnCl_4]_{eff}$ = $[SnCl_4]$ − [Lu].

and the presence of dimeric counterion ($Sn_2Cl_9^-$) during the polymerizations. However, this finding is in contradiction with the first-order dependence on Lewis acid obtained for the $SnCl_4$-,[48,67,68] BCl_3-,[69] or $B(C_6F_5)_3$[64,70]-co-initiated cationic polymerization of related styrenic monomers. This contradiction could be resolved by taking into account the formation of a complex between 2,6-lutidine and $SnCl_4$[71−73] that leads to the decrease of concentration of Lewis acid. A similar effect was also reported by Storey and Donnalley for $TiCl_4$-coinitiated cationic polymerization of isobutylene in the presence of 2,4-dimethylpyridine.[74] Indeed, the correction of $SnCl_4$ concentration by the concentration of 2,6-lutidine as $[SnCl_4]_{eff}$ = $[SnCl_4]$ − [Lu] (where $[SnCl_4]_{eff}$ is the effective concentration of $SnCl_4$) results in expected first-order dependence and the presence of monomeric ($SnCl_5^-$) counterion during the cationic polymerization of anethole polymerization (Figure 8).

PAn Characterization. The structure of PAn synthesized with the CumCl/$SnCl_4$/2,6-lutidine initiating system was studied by ^{1}H NMR spectroscopy. The broad resonances of protons of main-chain methyl and methine groups were observed at 0.02−1.16 and 1.18−2.47 ppm, while the signals at 3.37−3.99 and 5.31−7.08 ppm were assigned to protons of methoxy group and aromatic protons, respectively (Figure 9a). However, the signals of protons in the head and end groups cannot be detected by ^{1}H NMR spectroscopy due to their overlapping with the main-chain signals. Therefore, MALDI-TOF MS was used to analyze the terminal structure of the synthesized PAns (Figure 9b). The major population of peaks in PAn synthesized with CumCl as the initiator is clearly separated from each other by a molecular weight of the monomer unit and corresponds to the polymer chain bearing cumyl head and olefinic end groups, respectively, cationized by Na^+ (M_n = 2660.53 g mol^{-1}, n = 17) (Figure 9b). The minor population with higher molecular weight (+46 m/z) can be attributed to PAn with a terminal ethoxy group (Figure 9b), which appeared due to quenching reaction mixture by ethanol. The presence of an ethoxy end group in the polymer is also confirmed by ^{1}H NMR spectroscopy, where the signal of protons of the O$\underline{CH_2}$ group was detected at 2.90 ppm. MALDI-TOF spectrum also showed a series of low-intensity peaks with +18 m/z, which are observed in the full range of detected masses (Figure 9b). The appearance of this population is attributed to OH-terminated polymer chains, which could be generated during deactivation of the polymerization or dissolution/precipitation procedures due to the presence of a small amount of H_2O in ethanol.

The predominant formation of a terminal double bond in PAn synthesized with the CumCl/$SnCl_4$/2,6-lutidine initiating system is quite unexpected in view of good control over polymerization confirmed by the linearity of first-order plots, a good correlation between experimental and theoretical molecular weights, and monomer addition experiment (*vide supra*). Therefore, the formation of a terminal olefinic group proceeds *via* HCl elimination from Cl-terminated PAn obtained in the course of reversible termination (see Scheme 2). The elimination may occur during the work up procedure as it was reported for poly(α-methylstyrene) obtained by living cationic polymerization[75] as well as in the course of MALDI-TOF MS analysis due to the quite low stability of benzylic halogen terminus upon laser ionization in PSt and related polymers.[76]

This assumption is also confirmed by the analysis of the PAn obtained with the pMOSt−HCl/$SnCl_4$/2,6-lutidine initiating system. In order to demonstrate a dominant presence of a chlorine end group and its ability of alcoholysis, freshly synthesized polymer sample after quenching the reaction by ethanol was additionally stirred for 24 h at room temperature. As a result, the MALDI-TOF MS analysis of this PAn revealed

https://doi.org/10.1021/acssuschemeng.1c01504
ACS Sustainable Chem. Eng. 2021, 9, 6841−6854

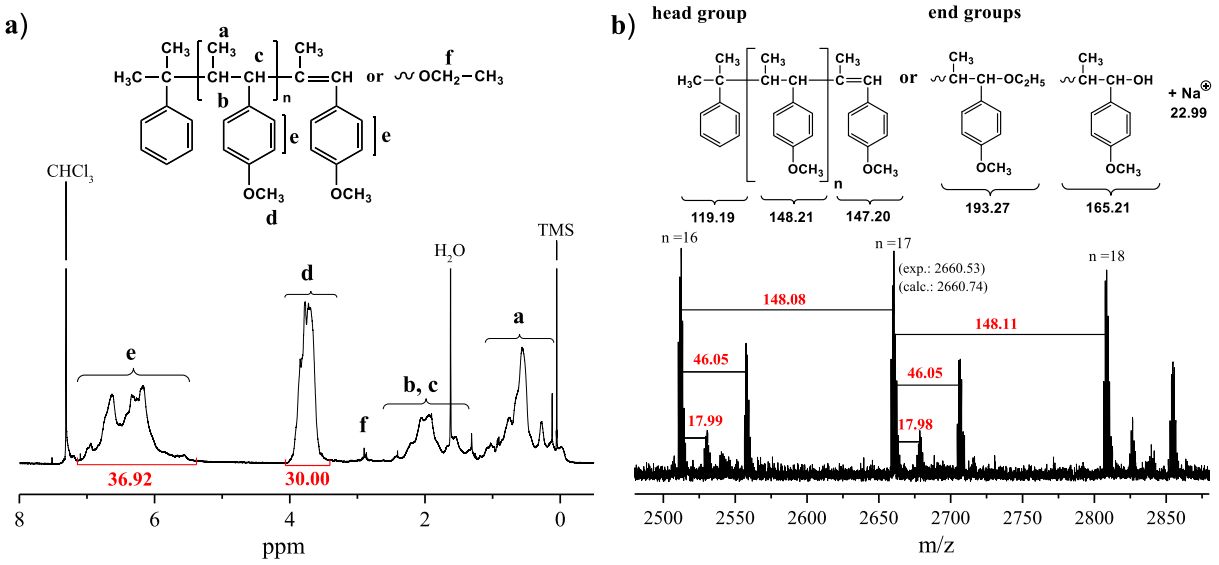

Figure 9. (a) ^{1}H NMR spectrum and (b) MALDI-TOF mass spectrum of PAn (M_n = 5100 g mol^{-1}, $Đ$ = 1.23, ω = 8%) synthesized with the CumCl/$SnCl_4$/2,6-lutidine initiating system in toluene at −60 °C.

Scheme 2. Tentative Mechanism of Cationic Polymerization of Anethole with the CumCl/$SnCl_4$/2,6-Lutidine Initiating System

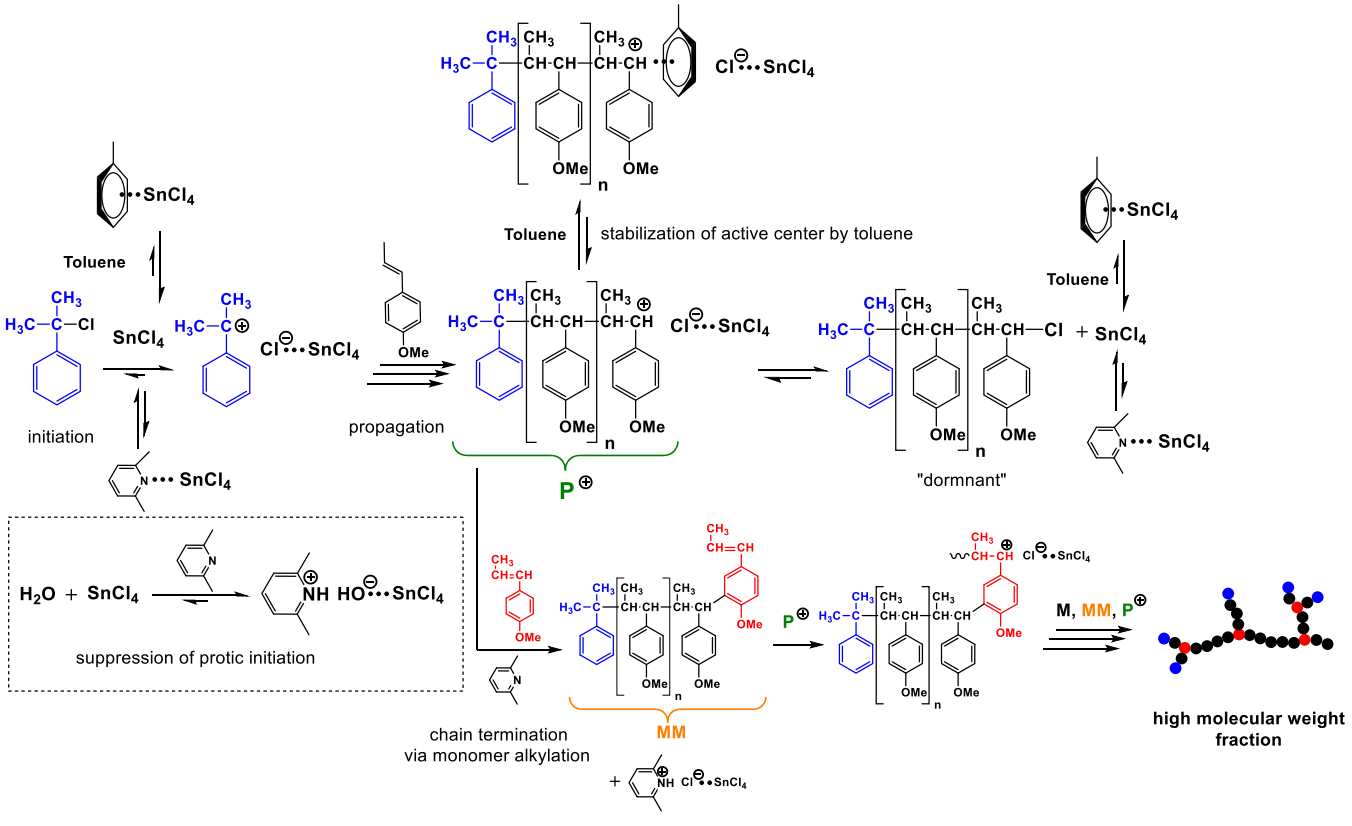

the dominant population of peaks corresponding to the polymer bearing the fragment of the initiator at the one side of the chain and ethoxy group at the other side of the chain cationized by Na^+ (M_n = 6281.476 g mol^{-1}, n = 40) (Figure 10a). Indeed, as it was previously shown, the termination of the cationic polymerization of the structurally similar monomer (pMOSt) by methanol results in the formation of a methoxy end group due to the methanolysis of the chlorine-terminated poly(pMOSt).[48] The population corresponding to PAn with a terminal olefinic group (−46 m/z) was still detected in the spectrum, but the intensity of such signals was very low (Figure 10a). As in the case of using CumCl, the low-intensity peaks assigned to the hydroxyl-terminated polymer were also identified in the structure of PAn obtained with pMOSt−HCl as the initiator. Finally, MALDI-TOF mass spectrum of PAn synthesized with MSA as the initiator, as anticipated, was poorly resolved and characterized by many different populations of peaks in the low-molecular-weight

https://doi.org/10.1021/acssuschemeng.1c01504
ACS Sustainable Chem. Eng. 2021, 9, 6841−6854

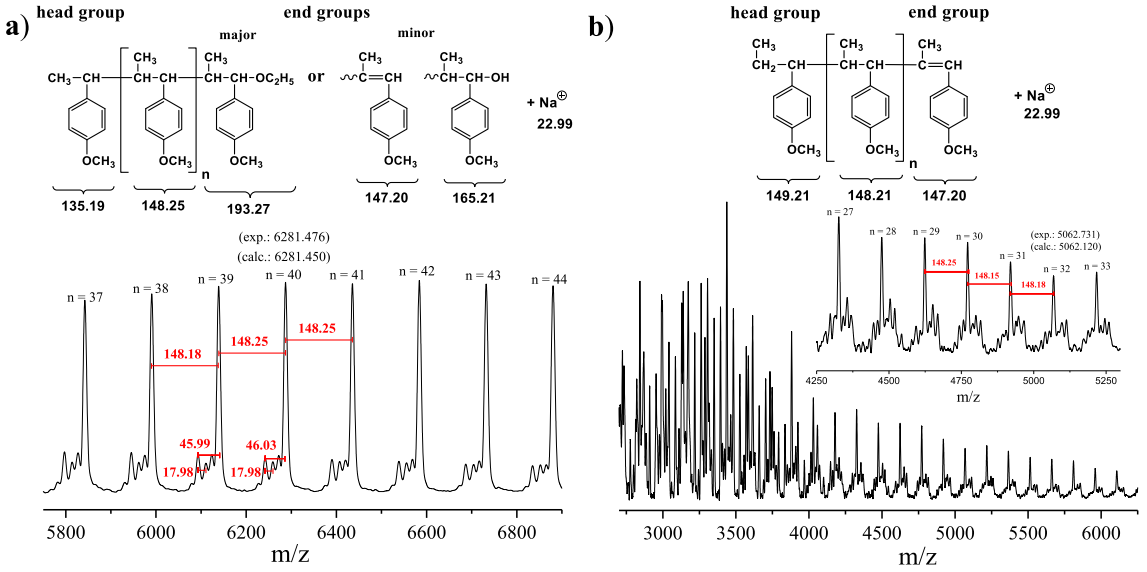

Figure 10. MALDI-TOF spectra of PAns synthesized with (a) pMOSt–HCl (M_n = 6100 g mol^{-1}; $Đ$ = 1.28; ω = 11%) and (b) MSA (M_n = 8700 g mol^{-1}; $Đ$ = 2.78; ω = 0%) as initiators.

region (Figure 10b) due to the nonliving nature of the polymerization. Nevertheless, the major population of the peaks corresponded to the polymer chains generated *via* proton initiation and terminated *via* chain-transfer to the monomer (Figure 10b).

Mechanism of Polymerization. Based on the obtained results, the tentative mechanism of the quasiliving cationic polymerization of anethole with a CumCl/$SnCl_4$/2,6-lutidine initiating system is proposed (Scheme 2). After generation of cumyl cation upon the interaction of $SnCl_4$ with CumCl, monomer molecules were added to this cation until reversible termination with the formation of dormant polymer chains occurred. The additional stabilization of active species might occur through their interaction with toluene (Scheme 2). This stabilization in conjunction with the reversible formation of a dormant polymer chain provides control over polymerization. As was mentioned above, another role of toluene in cationic polymerization consists of the formation of a weak complex with the Lewis acid, thus modifying its acidity. In addition, protic initiation due to the presence of traces of water in the system is totally prevented by the complexation of protons with 2,6-lutidine (Scheme 2). It should be noted that 2,6-lutidine can also form a strong complex with $SnCl_4$, thus decreasing the effective concentration of the Lewis acid.

However, despite the good control over the $SnCl_4$-coinitiated cationic polymerization of anethole achieved in this work, the polymerization process is invariably accompanied by the formation of a high-molecular-weight fraction. Even at the best conditions reported in this work, the content of the high-molecular-weight fraction is about 8%. After careful analysis of all experimental data, it was proposed that chain transfer to monomer *via* monomer alkylation occurs in the $SnCl_4$-coinitiated cationic polymerization of anethole as the main side reaction, which is responsible for the generation of a branched polymer (high-molecular-weight fraction) (Scheme 2). This side reaction proceeds *via* the formation of a macromonomer (MM in Scheme 2) in the course of alkylation of anethole followed by its copolymerization with anethole/other MM, finally generating branched polymeric structures. Protons formed during the alkylation process are successfully trapped by 2,6-lutidine (Scheme 2) confirmed by the observed curvature of the first-order plot [visible only for experiments where polymers containing high amount of the high-molecular-weight fraction are formed (Figures 5a and S8a)] in the presence of a proton trap as compared to linear kinetics for the experiment performed without the addition of a proton trap (Figure S8). Both the appearance of the high-molecular-weight fraction even at low monomer conversion (*vide supra*) and the gradual increase of M_n of the high-molecular-weight fraction with increasing monomer conversion indicate that the side reaction proceeds simultaneously with a propagation.

Such unusual chain transfer to the monomer *via* its alkylation in cationic polymerization of anethole could be explained by nontypical distribution of the partial negative charge on the molecule. Indeed, DFT calculations revealed that carbon atom at the β-position in the vinyl group of anethole is characterized by a much lower negative charge in comparison with aromatic carbon atoms in the ortho-position to methoxy group (Figure 11), that is, aromatic carbon atoms

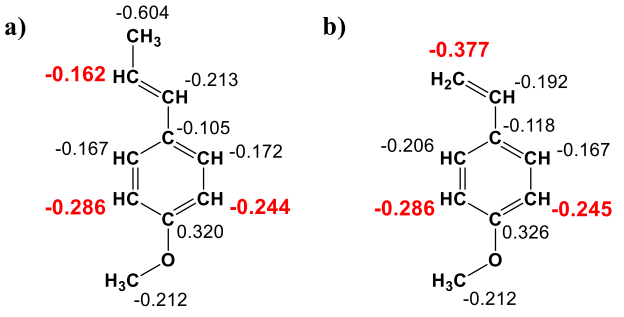

Figure 11. NBO charges at carbon atoms in (a) anethole and (b) pMOSt.

possessing higher electronic density are energetically more preferable for interaction with cationic species, on the one hand. On the other hand, due to steric hindrance, the addition to double bond of the monomer evidently predominates over the monomer alkylation. It should be admitted that a similar effect was previously reported for $SnCl_4$-coinitiated cationic

https://doi.org/10.1021/acssuschemeng.1c01504
ACS Sustainable Chem. Eng. 2021, 9, 6841–6854

Table 2. Thermal and Mechanical Properties of PAns Synthesized with the DiCumCl/$SnCl_4$/2,6-Lutidine Initiating System

entry	polymer	M_n (g mol^{-1})	$Đ$	ω[a] (%)	T_g[b] (°C)	T_{d5}[c] (°C)	E (GPa)
1	PAn	10,200	1.26	9	218.2	384.2	
2	PAn	15,900	1.31	16	245.8	384.1	
3	PAn	23,700	1.52	16	255.5	385.7	3.1 ± 0.5[d]
4	PSt	83,700	2.29		105[e]	362[e]	2.4−3.2[f]
5	PMMA	120,000[g]			109[e]	318[e]	2.4−3.3[f]

[a]Content of the high-molecular-weight fraction calculated from SEC curves. [b]Glass transition temperature (T_g) was determined by DSC analysis. [c]5% weight loss temperature (T_{d5}) was determined by TGA. [d]The Young's modulus (E) was determined by AFM method. [e]According to the literature (ref 13). [f]According to the literature (ref 81). [g]Weight-average molecular weight.

polymerization of 9-(4-vinylphenyl)carbazole, where low electronic density on the carbon on double bond resulted in the proceeding polymerization predominantly *via* step-growth pathway through addition of protonated monomer/oligomers to 3-position of carbazolyl group (electrophilic aromatic substitution).[77] Along with steric effect of the methyl group,[42] the observed charge distribution in anethole can also be a good explanation of much lower reactivity of anethole in cationic polymerization compared to a structurally similar pMOSt possessing the highest negative charge on vinyl group (Figure 11). Indeed, the rate of monomer consumption is more than 200 times higher for pMOSt than for An polymerization under the same conditions (Table S5).

In order to demonstrate that only alkylation of monomer, but not intermolecular alkylation (chain transfer to polymer), which is a typical side reaction in cationic polymerization of styrene, took place during $SnCl_4$-coinitiated cationic polymerization of anethole, the evolution of M_n, $Đ$ and ω with reaction time under monomer-starved conditions was investigated. As evident from Figure S9a, no change in shape of SEC curves or content of the high-molecular-weight fraction was observed for PAn even after keeping the non-quenched reaction mixture in the absence of a monomer for 1.5 h. The similar absence of intermolecular alkylation was also observed for the poly(pMOSt) under similar experimental conditions (Figure S9b). Another evidence supporting the occurrence of monomer alkylation consists of the reduced content of aromatic protons in ^{1}H NMR spectra as compared to theoretical value: [I(e)/I(d) = 3.69/3.00 (experimental) and I(e)/I(d) = 4.00/3.00 (theoretical) (Figure 9a, Table S6)].

Properties. In order to evaluate thermal and mechanical properties of the synthesized PAns, several samples of polymers with different molecular weights were synthesized with the DiCumCl/$SnCl_4$/2,6-lutidine initiating system (Table 2). First, the glass transition temperature (T_g) of the samples was determined using DSC. It should be noted that PAns are characterized by quite high values of glass transition temperature (Table 2), which are more than 2 times higher than the T_g of such a structurally similar polymer to poly(pMOSt) (T_g = 104−112 °C).[78,79] This result clearly suggests that kinetic rigidity of polymer chains significantly increases with the appearance of methyl groups in β-position. As it was anticipated, the T_g values decreased with decreasing molecular weight, still remaining very high (T_g = 218 °C) even for a polymer with M_n ∼ 10,000 g mol^{-1} (Figures S10−S12). It should also be noted that the determined T_g values are close to the one reported for PAn (M_n = 17,200 g mol^{-1} and $Đ$ = 4.32) obtained by conventional cationic polymerization using a complex of $AlCl_3$·Ph_2O as coinitiator (T_g = 249.9 °C).[80] The 5% weight loss temperature (T_{d5}) determined by TGA also revealed the high thermal stability of synthesized polymers (T_{d5} = 384.1−385.7 °C) (Table 2, Figure S13). The observed values demonstrate better thermal stability of PAn in comparison with industrially produced plastics, such as PSt (T_{d5} = 362 °C) and poly(methyl methacrylate) (PMMA) (T_{d5} = 318 °C).

Due to the high brittleness of PAn, the Young's modulus (E) was estimated using AFM. The measurements displayed a value of 3.1 ± 0.5 GPa that is comparable with the same parameter for commercially available PSt (E = 2.4−3.2 GPa) and PMMA (E = 2.4−3.3 GPa) (Table 2).

Taking into account the fact that anethole demonstrates antimicrobial activity against various microorganisms,[82,83] we have estimated briefly the ability of bacteria to grow on the PAn surface. Microbiological tests were carried out using *E. coli* as representative Gram-negative bacteria. The test consists of qualitative evaluation of total bacteria volume formed at a polymer film surface (PSt was used as a reference) after *E. coli* was cultivated for 24 h. It was demonstrated that bacteria adhesion is considerably lower for PAn films (less than 40% of the surface was covered by the cells) as compared to PSt films where a dense layer of bacteria was formed (Figure S14). This feature of PAn makes the polymer promising for application in food packaging. Further tests are required to clarify the possible molecular mechanism of the observed effect and to evaluate the activity of other abundant microorganisms toward polyanethole.

CONCLUSIONS

In this work, we reported *for the first time* the synthesis of well-defined polymers from such biomass-derived monomers as anethole *via* quasiliving cationic polymerization in toluene as the solvent. The use of toluene, which can stabilize the active species *via* weak interaction and modulate the Lewis acidity of the coinitiator ($SnCl_4$), and the addition of a proton trap are key points to achieve control over the polymerization process. However, despite good control over the $SnCl_4$-coinitiated cationic polymerization of anethole, the polymerization process was invariably accompanied by the formation of the high-molecular-weight fraction. The chain transfer to monomer (monomer alkylation), which proceeds simultaneously with the propagation, was responsible for the formation of the high-molecular-weight fraction. According to DFT calculations, this feature of the cationic polymerization of anethole, in contrast to other styrene derivatives, is consistent with the lower electronic density on the vinyl group than in ortho position toward the methoxy group of the benzene moiety of the monomer. Nevertheless, the CumCl/$SnCl_4$/2,6-lutidine or DiCumCl/$SnCl_4$/2,6-lutidine initiating system under optimized conditions (toluene as solvent, temperature from −50 to −60 °C) induced quasiliving cationic polymerization of anethole, affording polymers with M_n up to 24,000 g mol^{-1} and

https://doi.org/10.1021/acssuschemeng.1c01504
ACS Sustainable Chem. Eng. 2021, 9, 6841−6854

low polydispersity ($Đ$ < 1.31) containing a low amount of the high-molecular-weight fraction (8−15%). Finally, the synthesized PAns were characterized by high glass transition temperature (T_g > 220 °C), high thermal stability (T_{d5} > 385 °C), and high Young's modulus 3.1 ± 0.5 GPa that makes them promising to be used as high-performance plastic for some specific applications and to be regarded as a more sustainable alternative for common commodity polymers from petrochemicals (for instance, PSt and PMMA). In addition, PAn was found to demonstrate a certain resistance to bacterial growth on its surface compared to commercially available PSt.

■ ASSOCIATED CONTENT

Supporting Information

The Supporting Information is available free of charge at https://pubs.acs.org/doi/10.1021/acssuschemeng.1c01504.

Results of anethole cationic polymerization in the presence of Bu_4NBr as an additive, polymer fractionation by preparative SEC, different initiators (MSA, pMOSt−HCl, and DiCumCl), kinetics and M_n, $Đ$ versus conversion plots, SEC traces of PAns and poly(pMOSt)s synthesized under monomer-starved conditions, DSC and TGA curves of PAns, and microphotographs of polymer films surface with bacteria (PDF)

■ AUTHOR INFORMATION

Corresponding Author

Sergei V. Kostjuk − *Research Institute for Physical Chemical Problems of the Belarusian State University, Minsk 220006, Belarus; Department of Chemistry, Belarusian State University, Minsk 220006, Belarus; Institute for Regenerative Medicine, Sechenov First Moscow State Medical University, Moscow 119991, Russia;* orcid.org/0000-0002-7466-3662; Email: kostjuks@bsu.by

Authors

Maksim I. Hulnik − *Research Institute for Physical Chemical Problems of the Belarusian State University, Minsk 220006, Belarus; Department of Chemistry, Belarusian State University, Minsk 220006, Belarus*

Olga V. Kuharenko − *Research Institute for Physical Chemical Problems of the Belarusian State University, Minsk 220006, Belarus; Department of Chemistry, Belarusian State University, Minsk 220006, Belarus*

Irina V. Vasilenko − *Research Institute for Physical Chemical Problems of the Belarusian State University, Minsk 220006, Belarus*

Peter Timashev − *Institute for Regenerative Medicine, Sechenov First Moscow State Medical University, Moscow 119991, Russia; World-Class Research Center "Digital Biodesign and Personalized Healthcare", Sechenov First Moscow State Medical University (Sechenov University), Moscow 119991, Russia; N.N. Semenov Federal Research Center for Chemical Physics, RAS, Moscow 119991, Russia; Chemistry Department, Lomonosov Moscow State University, Moscow 119991, Russian Federation*

Complete contact information is available at: https://pubs.acs.org/10.1021/acssuschemeng.1c01504

Notes

The authors declare no competing financial interest.

■ ACKNOWLEDGMENTS

This work was financed by the Ministry of Science and Higher Education of the Russian Federation within the framework of state support for the creation and development of World-Class Research Centers "Digital biodesign and personalized healthcare" no. 075-15-2020-926 and, in part, by the State Belarusian Program of Scientific Research "Chemical technologies and materials" subprogram "Wood chemistry", project 4.1.12. We are grateful to Dr. Y. Efremov (Institute for Regenerative Medicine), Dr. Y. Falterov (Belarusian State University), and Dr. P. Nikishau (Research Institute for Physical Chemical Problems of the Belarusian State University) for nanomechanic measurements, microbiologic tests, and DFT calculations, respectively.

■ REFERENCES

(1) Zhu, Y.; Romain, C.; Williams, C. K. Sustainable Polymers from Renewable Resources. *Nature* **2016**, *540*, 354−362.

(2) Meier, M. A. R.; Metzger, J. O.; Schubert, U. S. Plant Oil Renewable Resources as Green Alternatives in Polymer Science. *Chem. Soc. Rev.* **2007**, *36*, 1788−1802.

(3) Williams, C.; Hillmyer, M. Polymers from Renewable Resources: A Perspective for a Special Issue of Polymer Reviews. *Polym. Rev.* **2008**, *48*, 1−10.

(4) Schröder, K.; Matyjaszewski, K.; Noonan, K. J. T.; Mathers, R. T. Towards Sustainable Polymer Chemistry with Homogeneous Metal-Based Catalysts. *Green Chem.* **2014**, *16*, 1673−1686.

(5) Holmberg, A. L.; Reno, K. H.; Wool, R. P.; Epps, T. H., III Biobased Building Blocks for the Rational Design of Renewable Block Polymers. *Soft Matter* **2014**, *10*, 7405−7424.

(6) Gandini, A.; Lacerda, T. M. From Monomers to Polymers from Renewable Resources: Recent Advances. *Prog. Polym. Sci.* **2015**, *48*, 1−39.

(7) Winnacker, M.; Rieger, B. Recent Progress in Sustainable Polymers Obtained from Cyclic Terpenes: Synthesis, Properties, and Application Potential. *ChemSusChem* **2015**, *8*, 2455−2471.

(8) Satoh, K. Controlled/Living Polymerization of Renewable Vinyl Monomers into Bio-Based Polymers. *Polym. J.* **2015**, *47*, 527−536.

(9) Llevot, A.; Dannecker, P.-K.; von Czapiewski, M.; Over, L. C.; Söyler, Z.; Meier, M. A. R. Renewability is not Enough: Recent Advances in the Sustainable Synthesis of Biomass-Derived Monomers and Polymers. *Chem.—Eur. J.* **2016**, *22*, 11510−11521.

(10) Thomsett, M. R.; Storr, T. E.; Monaghan, O. R.; Stockman, R. A.; Howdle, S. M. Progress in the Synthesis of Sustainable Polymers from Terpenes and Terpenoids. *Green Mater.* **2016**, *4*, 115−134.

(11) Sahu, P.; Bhowmick, A. K.; Kali, G. Terpene Based Elastomers: Synthesis, Properties, and Applications. *Processes* **2020**, *8*, 553.

(12) Shin, J.; Lee, Y.; Tolman, W. B.; Hillmyer, M. A. Thermoplastic Elastomers Derived from Menthide and Tulipalin A. *Biomacromolecules* **2012**, *13*, 3833−3840.

(13) Satoh, K.; Nakahara, A.; Mukunoki, K.; Sugiyama, H.; Saito, H.; Kamigaito, M. Sustainable Cycloolefin Polymer from Pine Tree Oil for Optoelectronics Material: Living Cationic Polymerization of β-Pinene and Catalytic Hydrogenation of High-Molecular-Weight Hydrogenated Poly(β-Pinene). *Polym. Chem.* **2014**, *5*, 3222−3230.

(14) Hauenstein, O.; Reiter, M.; Agarwal, S.; Rieger, B.; Greiner, A. Bio-Based Polycarbonate from Limonene Oxide and CO_2 with High Molecular Weight, Excellent Thermal Resistance, Hardness and Transparency. *Green Chem.* **2016**, *18*, 760−770.

(15) Raza, S.; Yong, X.; Yang, B.; Xu, R.; Deng, J. Biomass trans-Anethole-Based Hollow Polymer Particles: Preparation and Application as Sustainable Absorbent. *ACS Sustainable Chem. Eng.* **2017**, *5*, 10011−10018.

(16) Sahu, P.; Bhowmick, A. K. Sustainable Self-Healing Elastomers with Thermoreversible Network Derived from Biomass via Emulsion Polymerization. *J. Polym. Sci., Part A: Polym. Chem.* **2019**, *57*, 738−751.

(17) Kuznetsova, D.; Ageykin, A.; Koroleva, A.; Deiwick, A.; Shpichka, A.; Solovieva, A.; Kostjuk, S.; Meleshina, A.; Rodimova, S.; Akovanceva, A.; Butnaru, D.; Frolova, A.; Zagaynova, E.; Chichkov, B.; Bagratashvili, V.; Timashev, P. Surface Micromorphology of Cross-Linked Tetrafunctional Polylactide Scaffolds Inducing Vessel Growth and Bone Formation. *Biofabrication* **2017**, *9*, 025009.
(18) Timashev, P.; Kuznetsova, D.; Koroleva, A.; Prodanets, N.; Deiwick, A.; Piskun, Y.; Bardakova, K.; Dzhoyashvili, N.; Kostjuk, S.; Zagaynova, E.; Rochev, Y.; Chichkov, B.; Bagratashvili, V. Novel Biodegradable Star-Shaped Polylactide Scaffolds for Bone Regeneration Fabricated by Two-Photon Polymerization. *Nanomedicine* **2016**, *11*, 1041−1053.
(19) Salvin, S.; Bourke, M.; Byrne, T. *The New Crop Industries Handbook*; Rural Industries Research and Development Corporation: Canberra, Australia, 2004.
(20) Odian, G. *Principles of Polymerization*, 4th ed.; Wiley-Interscience: Hoboken, NJ, 2004; pp 201−202.
(21) Overberger, C. G.; Tanner, D.; Pearce, E. M. Ionic Polymerization. Copolymerization of Nuclear and Side-chain Alkyl-substituted Styrene Monomers. *J. Am. Chem. Soc.* **1958**, *80*, 4566−4568.
(22) Higashimura, T.; Kawamura, K.; Masuda, T. Cationic Copolymerization of Anethole: Reactivity of Geometric Isomers of a p-Disubstituted Ethylenes. *J. Polym. Sci., Polym. Chem. Ed.* **1972**, *10*, 85−93.
(23) Wang, C.; Sun, J.; Tao, Y.; Fang, L.; Zhou, J.; Dai, M.; Liu, M.; Fang, Q. Biomass Materials Derived from Anethole: Conversion and Application. *Polym. Chem.* **2020**, *11*, 954−963.
(24) Davis, M. C.; Guenthner, A. J.; Groshens, T. J.; Reams, J. T.; Mabry, J. M. Polycyanurate Networks from Anethole Dimers: Synthesis and Characterization. *J. Polym. Sci., Part A: Polym. Chem.* **2012**, *50*, 4127−4136.
(25) Davis, M. C.; Guenthner, A. J.; Sahagun, C. M.; Lamison, K. R.; Reams, J. T.; Mabry, J. M. Polycyanurate Networks from Dehydroanethole Cyclotrimers: Synthesis and Characterization. *Polymer* **2013**, *54*, 6902−6909.
(26) He, F.; Gao, Y.; Jin, K.; Wang, J.; Sun, J.; Fang, Q. Conversion of a Biorenewable Plant Oil (Anethole) to a New Fluoropolymer with Both Low Dielectric Constant and Low Water Uptake. *ACS Sustainable Chem. Eng.* **2016**, *4*, 4451−4456.
(27) He, F.; Jin, K.; Wang, Y.; Wang, J.; Zhou, J.; Sun, J.; Fang, Q. High Performance Polymer Derived from a Biorenewable Plant Oil (Anethole). *ACS Sustainable Chem. Eng.* **2017**, *5*, 2578−2584.
(28) Tao, Y.; He, F.; Jin, K.; Wang, J.; Wang, Y.; Zhou, J.; Sun, J.; Fang, Q. Facile Conversion of Plant Oil (Anethole) to a High-Performance Material. *Polym. Chem.* **2017**, *8*, 2010−2015.
(29) Braun, D.; Hu, F. Polymers from Non-Homopolymerizable Monomers by Free Radical Processes. *Prog. Polym. Sci.* **2006**, *31*, 239−276.
(30) Braun, D.; Hu, F. Free Radical Terpolymerization of Three Non-Homopolymerizable Monomers. Part IV. Terpolymerization of Maleic Anhydride, Trans-Anethole and Vinyl-iso-Butylether. *Polymer* **2004**, *45*, 61−70.
(31) Braun, D.; Hu, F. Free Radical Terpolymerization of Trans-Anethole, Maleic Anhydride and N-Ethylmaleimide. *J. Macromol. Sci., Part A: Pure Appl.Chem.* **2005**, *42*, 1127−1146.
(32) Nonoyama, Y.; Satoh, K.; Kamigaito, M. Renewable β-Methylstyrenes for Bio-Based Heat-Resistant Styrenic Copolymers: Radical Copolymerization Enhanced by Fluoroalcohol and Controlled/Living Copolymerization by RAFT. *Polym. Chem.* **2014**, *5*, 3182−3189.
(33) Yuan, Y.; Yong, X.; Zhang, H.; Deng, J. Biobased Microspheres Consisting of Poly(trans-anethole-co-maleic anhydride) Prepared by Precipitation Polymerization and Adsorption Performance. *ACS Sustainable Chem. Eng.* **2016**, *4*, 1446−1453.
(34) Raza, S.; Yong, X.; Raza, M.; Deng, J. Synthesis of Biomass Trans-Anethole Based Magnetic Hollow Polymer Particles and Their Applications as Renewable Adsorbent. *Chem. Eng. J.* **2018**, *352*, 20−28.
(35) Raza, S.; Yong, X.; Deng, J. Immobilizing Cellulase on Multi-Layered Magnetic Hollow Particles: Preparation, Bio-Catalysis and Adsorption Performances. *Microporous Mesoporous Mater.* **2019**, *285*, 112−119.
(36) Yong, X.; Wu, Y.; Deng, J. Chiral Helical Substituted Polyacetylene Grafted on Hollow Polymer Particles: Preparation and Enantioselective Adsorption Towards Cinchona Alkaloids. *Polym. Chem.* **2019**, *10*, 4441−4448.
(37) Higashimura, T.; Hirokawa, Y.; Matsuzaki, K.; Kawamura, T.; Uryu, T. Cationic Polymerization of Anethole and Its Model Reaction: A Stereochemical Approach to the Propagation Mechanism. *Polym. J.* **1979**, *11*, 855−862.
(38) Alexander, R.; Jefferson, A.; Lester, P. D. Cationic Oligomerization and Polymerization of Some Propenylbenzene Derivatives. *J. Polym. Sci., Polym. Chem. Ed.* **1981**, *19*, 695−706.
(39) Higashimura, T.; Hiza, M. Cationic Oligomerization of Anethole: Selective Synthesis of Dimers and Trimers. *J. Polym. Sci., Polym. Chem. Ed.* **1981**, *19*, 1957−1966.
(40) Higashimura, T.; Kawamura, K.; Masuda, T. Cationic Copolymerization of Anethole: Reactivity of Geometric Isomers of α,β-Disubstituted Ethylenes. *J. Polym. Sci., Polym. Chem. Ed.* **1972**, *10*, 85−93.
(41) Mizote, A.; Tanaka, T.; Higashimura, T.; Okamura, S. Cationic Polymerization α,β-Disubstituted Olefins. Part I. Cationic Copolymerization of β-Methylstyrenes. *J. Polym. Sci., Polym. Chem. Ed.* **1965**, *3*, 2567−2578.
(42) Satoh, K.; Saitoh, S.; Kamigaito, M. A Linear Lignin Analogue: Phenolic Alternating Copolymers from Naturally Occurring β-Methylstyrene via Aqueous-Controlled Cationic Copolymerization. *J. Am. Chem. Soc.* **2007**, *129*, 9586−9587.
(43) Hulnik, M. I.; Vasilenko, I. V.; Radchenko, A. V.; Peruch, F.; Ganachaud, F.; Kostjuk, S. V. Aqueous Cationic Homo- and Co-Polymerizations of β-Myrcene and Styrene: a Green Route Toward Terpene-Based Rubbery Polymers. *Polym. Chem.* **2018**, *9*, 5690−5700.
(44) Kukhta, N. A.; Vasilenko, I. V.; Kostjuk, S. V. Room Temperature Cationic Polymerization of β-Pinene Using Modified $AlCl_3$ Catalyst: Toward Sustainable Plastics from Renewable Biomass Resources. *Green Chem.* **2011**, *13*, 2362−2364.
(45) Storey, R. F.; Chisholm, B. J. Aspects of the Synthesis of Poly(styrene-b-isobutylene-b-styrene) Block Copolymers Using Living Carbocationic Polymerization. *Macromolecules* **1993**, *26*, 6727−6733.
(46) Becke, A. D. Density-Functional Thermochemistry. III. The Role of Exact Exchange. *J. Chem. Phys.* **1993**, *98*, 5648−5652.
(47) Cancès, E.; Mennucci, B.; Tomasi, J. A New Integral Equation Formalism for the Polarizable Continuum Model: Theoretical Background and Applications to Isotropic and Anisotropic Dielectrics. *J. Chem. Phys.* **1997**, *107*, 3032−3041.
(48) De, P.; Faust, R. Living Carbocationic Polymerization of p-Methoxystyrene Using p-Methoxystyrene Hydrochloride/$SnBr_4$ Initiating System: Determination of the Absolute Rate Constant of Propagation for Ion Pairs. *Macromolecules* **2004**, *37*, 7930−7937.
(49) Fodor, Z.; Gyor, M.; Wang, H.-C.; Faust, R. Living Carbocationic Polymerization of Styrene in the Presence of Proton Trap. *J. Macromol. Sci., Part A: Pure Appl.Chem.* **1993**, *30*, 349−363.
(50) Kali, G.; Szesztay, M.; Bodor, A.; Iván, B. A New Synthetic Method for the Preparation of Star-Shaped Polyisobutylene with Hyperbranched Polystyrene Core. *Macromol. Chem. Phys.* **2007**, *208*, 1388−1393.
(51) Kali, G.; Szesztay, M.; Bodor, A.; Iván, B. Star and Hyperbranched Polyisobutylenes via Terminally Reactive Polyisobutylene-Polystyrene Block Copolymers. *Macromol. Symp.* **2013**, *323*, 37−41.
(52) Higashimura, T.; Ishihama, Y.; Sawamoto, M. Living Cationic Polymerization of Styrene: New Initiating Systems Based on Added Halide Salts and the Nature of the Growing Species. *Macromolecules* **1993**, *26*, 744−751.

https://doi.org/10.1021/acssuschemeng.1c01504
ACS Sustainable Chem. Eng. 2021, 9, 6841−6854

(53) Kojima, K.; Sawamoto, M.; Higashimura, T. Living Cationic Polymerization of p-Methoxystyrene by the Hydrogen Iodide/Zinc Iodide and Hydrogen Iodide/Iodine Initiating Systems: Effects of Tetrabutylammonium Halides in a Polar Solvent. *Macromolecules* **1990**, *23*, 948−953.
(54) Miyashita, K.; Kamigaito, M.; Sawamoto, M.; Higashimura, T. End-Functionalized Polymers of Styrene and p-Methylstyrene by Living Cationic Polymerization with Functionalized Initiators. *Macromolecules* **1994**, *27*, 1093−1098.
(55) Nagy, A. s.; Majoros, I. n.; Kennedy, J. P. Living Carbocationic Polymerization. LXII. Living Polymerization of Styrene, p-Methylstyrene and p-Chlorostyrene Induced by the Common Ion Effect. *J. Polym. Sci., Part A: Polym. Chem.* **1997**, *35*, 3341−3347.
(56) Kanaoka, S.; Eika, Y.; Sawamoto, M.; Higashimura, T. Living Cationic Polymerization of p-Chlorostyrene and Related Para-Substituted Styrene Derivatives at Room Temperature. *Macromolecules* **1996**, *29*, 1778−1783.
(57) Kwon, O.-S.; Kim, Y.-B.; Kwon, S.-K.; Choi, B.-S.; Choi, S.-K. Living Cationic Polymerization of Styrene by 1-Chloroethylbenzene/Tin(IV) Chloride in Chloroform. *Makromol. Chem.* **1993**, *194*, 251−257.
(58) Vasilenko, I. V.; Nikishev, P. A.; Shiman, D. I.; Kostjuk, S. V. Cationic Polymerization of Isobutylene in Toluene: Toward Well-Defined Exo-Olefin Terminated Medium Molecular Weight Polyisobutylenes Under Mild Conditions. *Polym. Chem.* **2017**, *8*, 1417−1425.
(59) Berezianko, I. A.; Vasilenko, I. V.; Kostjuk, S. V. Cationic Polymerization of Isobutylene Co-initiated by Chloroferrate Imidazole-Based Ionic Liquid: The Advantageous Effect of Initiator and Aromatic Compounds. *Eur. Polym. J.* **2019**, *121*, 109307.
(60) Karasawa, Y.; Kimura, M.; Kanazawa, A.; Kanaoka, S.; Aoshima, S. New Initiating Systems for Cationic Polymerization of Plant-Derived Monomers: $GaCl_3$/Alkylbenzene-Induced Controlled Cationic Polymerization of β-Pinene. *Polym. J.* **2015**, *47*, 152−157.
(61) Fodor, Z.; Bae, Y. C.; Faust, R. Temperature Effects on the Living Cationic Polymerization of Isobutylene: Determination of Spontaneous Chain-Transfer Constants in the Presence of Terminative Chain Transfer. *Macromolecules* **1998**, *31*, 4439−4446.
(62) Bae, Y. C.; Faust, R. β-Proton Elimination by Free Bases in the Living Carbocationic Polymerization of Isobutylene. *Macromolecules* **1997**, *30*, 7341−7344.
(63) Held, D.; Iván, B.; Müller, A. H. E.; de Jong, F.; Graafland, T. Stability of Propagating Species in Living Cationic Polymerization of Isobutylene. *ACS Symp. Ser.* **1997**, *665*, 63−74.
(64) Kostjuk, S. V. Cationic Polymerization of p-Methoxystyrene Co-initiated by $B(C_6F_5)_3$: Effect of Acetonitrile and Proton Traps. *Eur. Polym. J.* **2020**, *129*, 109632.
(65) Lide, D. R. *CRC Handbook of Chemistry and Physics*, 75th ed.; CRC Press Inc.: Boca Raton, FL, 1994−1995.
(66) Radchenko, A. V.; Kostjuk, S. V.; Vasilenko, I.V.; Ganachaud, F.; Kaputsky, F. N. Controlled/Living Cationic Polymerization of Styrene with BF_3OEt_2 as a Coinitiator in the Presence of Water: Improvements and Limitations. *Eur. Polym. J.* **2007**, *43*, 2576−2583.
(67) De, P.; Faust, R. Determination of the Absolute Rate Constant of Propagation for Ion Pairs in the Cationic Polymerization of p-Methylstyrene. *Macromolecules* **2005**, *38*, 5498−5505.
(68) De, P.; Faust, R.; Schimmel, H.; Ofial, A. R.; Mayr, H. Determination of Rate Constants in the Carbocationic Polymerization of Styrene: Effect of Temperature, Solvent Polarity, and Lewis Acid. *Macromolecules* **2004**, *37*, 4422−4433.
(69) De, P.; Sipos, L.; Faust, R.; Moreau, M.; Charleux, B.; Vairon, J.-P. Determination of the Propagation Rate Constant in the Carbocationic Polymerization of 2,4,6-Trimethylstyrene. *Macromolecules* **2005**, *38*, 41−46.
(70) Kostjuk, S. V.; Radchenko, A. V.; Ganachaud, F. Controlled cationic polymerization of cyclopentadiene with $B(C_6F_5)_3$ as a coinitiator in the presence of water. *J. Polym. Sci., Part A: Polym. Chem.* **2008**, *46*, 4734−4747.
(71) Kennedy, J. P.; Ivan, B. *Designed Polymers by Carbocationic Macromolecular Engineering: Theory and Practice*; Hanser Publishers: Munich, 1992.
(72) Iván, B.; Szanka, I.; Szabó, Á.; Pásztor, S.; Pásztói, B.; Stumphauser, T.; Kasza, G.; Szarka, G.; Kalocsai, D.; Bajcsi, Á.; Fecske, D.; Kovács, E.; Osváth, Z.; Petróczy, A.; Verebélyi, K. Endfunctional polyisobutylenes by quasiliving carbocationic polymerization and bi-and multicomponent macromolecular architectures therefrom. In *Macromolecular Engineering: Design, Synthesis and Application of Polymers*; Lubnin, A., Erdodi, G., Eds.; Elsevier, 2021; pp 23−49.
(73) Dunstan, P. O. Thermochemistry of Adducts of Tin(IV) Chloride with Heterocyclic Bases. *Thermochim. Acta* **2003**, *398*, 1−7.
(74) Storey, R. F.; Donnalley, A. B. $TiCl_4$ Reaction Order in Living Isobutylene Polymerization at Low $[TiCl_4]$:[Chain End] Ratios. *Macromolecules* **2000**, *33*, 53−59.
(75) Higashimura, T.; Kamigaito, M.; Kato, M.; Hasebe, T.; Sawamoto, M. Living Cationic Polymerization of .Alpha.-Methylstyrene Initiated with a Vinyl Ether-Hydrogen Chloride Adduct inConjunction with Tin Tetrabromide. *Macromolecules* **1993**, *26*, 2670−2673.
(76) Nonaka, H.; Ouchi, M.; Kamigaito, M.; Sawamoto, M. MALDI-TOF-MS Analysis of Ruthenium(II)-Mediated Living Radical Polymerizations of Methyl Methacrylate, Methyl Acrylate, and Styrene. *Macromolecules* **2001**, *34*, 2083−2088.
(77) Vasilenko, I. V.; Vaitusionak, A. A.; Sutaite, J.; Tomkeviciene, A.; Ostrauskaite, J.; Grazulevicius, J. V.; Kostjuk, S. V. Simultaneous Step-Growth and Chain-Growth Cationic Polymerization of Styrenic Monomers Bearing Carbazolyl Groups. *Polymer* **2017**, *129*, 83−91.
(78) Vasilenko, I. V.; Yeong, H. Y.; Delgado, M.; Ouardad, S.; Peruch, F.; Voit, B.; Ganachaud, F.; Kostjuk, S. V. A Catalyst Platform for Unique Cationic (Co)Polymerization in Aqueous Emulsion. *Angew. Chem., Int. Ed.* **2015**, *54*, 12728−12732.
(79) Malhotra, S. L.; Lessard, P.; Blanchard, L. P. The Thermal Decomposition and Glass Transition Temperature of Poly-p-methoxystyrene. *J. Macromol. Sci., Chem.* **1981**, *15*, 301−321.
(80) Appiah-Ntiamoah, R.; Kim, H.; Gadisa, B. T.; Baye, A. F.; Abebe, M. W.; Kostjuk, S. V. Degradation Kinetics of Polyanethole: A Newly Synthesized Green Polymer. *Mater. Chem. Phys.* **2018**, *219*, 468−477.
(81) Ellis, B.; Smith, R. *Polymer: A Property Database*, 2nd ed.; CRC Press Inc.: Boca Raton, 2009.
(82) Auezova, L.; Najjar, A.; Kfoury, M.; Fourmentin, S.; Greige-Gerges, H. Antibacterial Activity of Free or Encapsulated Selected Phenylpropanoids Against Escherichia Coli and Staphylococcus Epidermidis. *J. Appl. Microbiol.* **2020**, *128*, 710−720.
(83) Kubo, I.; Fujita, K.-i.; Nihei, K.-i. Antimicrobial Activity of Anethole and Related Compounds from Aniseed. *J. Sci. Food Agric.* **2008**, *88*, 242−247.

https://doi.org/10.1021/acssuschemeng.1c01504
ACS Sustainable Chem. Eng. 2021, 9, 6841−6854